PCCP

Self-diffusivities in multicomponent mixtures in zeolites

R. Krishna and D. Paschek

Department of Chemical Engineering, University of Amsterdam, Nieuwe Achtergracht 166, 1018 WV Amsterdam, The Netherlands. E-mail: krishna@science.uva.nl; Tel: +31 20 5257007 Fax: +31 20 5255604

Received 17th January 2002, Accepted 1st March 2002
First published as an Advance Article on the web 15th April 2002

Using the Maxwell–Stefan formulation for diffusion in zeolites as a basis, we develop a general analytic expression for the self-diffusivity of a component in a multicomponent mixture. Correlation effects are accounted for by the introduction of particle–particle "exchange" coefficients. Various formulae for estimation of these exchange coefficients have been postulated. The developed procedure for estimation of the self-diffusivity is verified by comparison with kinetic Monte Carlo simulations for binary and ternary mixtures in MFI zeolite and in a square lattice. Additional verification of the analytic model is obtained using published molecular dynamics simulations and experimental data.

1. Introduction

Zeolites are widely used as adsorbents or catalysts in separation and reaction processes.[1–3] In the design of zeolite based processes, it is essential to have information on the diffusivities of the various components. While there are several experimental, and computational, studies on *single* species diffusion,[1,2] there is very little corresponding data on *mixture* diffusion. Snurr and Kärger[4] performed pulsed field gradient (PFG) NMR measurements and molecular dynamics (MD) simulations to determine self-diffusivities in a mixture of CH_4 and CF_4 in MFI zeolite. Jost *et al.*[5] performed similar studies for mixtures of CH_4 and xenon in MFI. Gergidis *et al.*[6,7] studied the self-diffusivities in a mixture of CH_4 and n-butane in MFI using molecular dynamics and quasi-elastic neutron scattering (QENS). Paschek and Krishna[8] used kinetic Monte Carlo (KMC) simulations to study self-diffusivities in a mixture of CH_4 and CF_4 in MFI. Schuring *et al.*[9] have determined the self-diffusivities in a mixture of n-hexane and 2-methylpentane in MFI using a tracer exchange positron emission profiling technique. There is no published data on self-diffusivities in mixtures containing three or more species.

Self-diffusivities in zeolites are strongly influenced by correlation effects associated with molecular jumps and, consequently, their values are lower than the "corrected", or Maxwell–Stefan diffusivities.[10,11] In order to predict self-diffusivities, we need to model correlation effects in *multi*component mixtures. No such model has been published yet.

The objectives of this work are two-fold. Firstly, we develop a general, analytic, expression for self-diffusivity of a component in a *multi*component mixture. The derivation uses the Maxwell–Stefan diffusion formulation as a basis. Correlation effects are taken account of by introducing particle–particle exchange coefficients; several approaches for estimation of these exchange coefficients are suggested. Secondly, we perform KMC simulations for self-diffusivities for diffusion of *binary* and *ternary* mixture in two types of lattices (see Fig. 1): (a) square lattice, and (b) MFI zeolite topology. These KMC simulations are used to validate the developed expression for self-diffusivities and to choose the appropriate model for estimation of the exchange coefficients. Further verification of the developed model is obtained using published MD mixture simulation data[4,6] and the experiments of Schuring *et al.*[9]

2. Development of theory for self-diffusivity

Consider n-component diffusion within a zeolite. The fluxes N_i can be related to the gradients of the fractional occupancies $\nabla\theta_i$ by the following relation by the generalized Fick's law:

$$(N) = -\rho[\Theta_{\mathrm{sat}}][D](\nabla\theta) \tag{1}$$

where $[D]$ is the n-dimensional square matrix of Fick diffusivities; ρ is the zeolite matrix density expressed as unit cells (or supercages) per m^3; $[\Theta_{\mathrm{sat}}]$ is a diagonal matrix with elements $\Theta_{i,\mathrm{sat}}$, representing the saturation loading of species i. The fractional occupancies θ_i are defined as:

$$\theta_i \equiv \Theta_i/\Theta_{i,\mathrm{sat}}; \quad i = 1, 2, \ldots n \tag{2}$$

where Θ_i represents the loading of species i expressed in molecules of sorbate (diffusant) per unit cell (or supercage).

For calculation of the fluxes N_i we need to estimate the $n \times n$ elements of $[D]$. The elements of $[D]$ are influenced not only by the species mobilities but also by the sorption thermody-

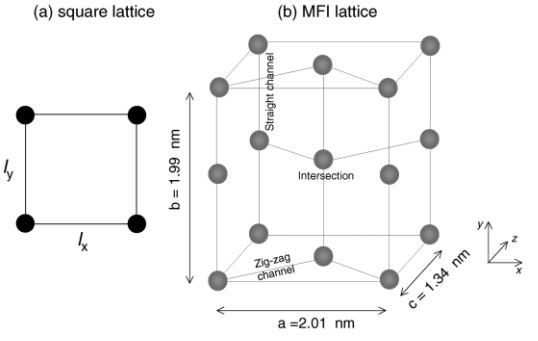

Fig. 1 Diffusion unit cells for (a) square lattice and (b) MFI. The large dots indicate the sorption sites.

namics. For estimating [$Đ$] it is necessary to use the Maxwell–Stefan formulation in which the chemical potential gradients are written as linear functions of the fluxes:[12–14]

$$-\rho\frac{\theta_i}{RT}\nabla\mu_i = \sum_{\substack{j=1\\ j\neq i}}^{n}\frac{\Theta_j N_i - \Theta_i N_j}{\Theta_{i,\mathrm{sat}}\Theta_{j,\mathrm{sat}}Đ_{ij}} + \frac{N_i}{\Theta_{i,\mathrm{sat}}Đ_i}; \quad i = 1,2,\ldots n \quad (3)$$

We have to reckon in general with two types of Maxwell–Stefan diffusivities: $Đ_i$ and $Đ_{ij}$. The $Đ_i$ are the diffusivities that reflect interactions between species i and the zeolite matrix; they are also referred to as jump or "corrected" diffusivities in the zeolite literature.[1–3] Experimental and MD simulation data[15] for weakly confined guest molecules in zeolitic hosts (*e.g.* methane in MFI) show that $Đ_i$ are practically independent of the loading, *i.e.*

$$Đ_i = Đ_i(0) \quad (4)$$

where $Đ_i(0)$ are the zero-loading diffusivities. For more strongly confined guest molecules, the M–S diffusivity decreases with the total occupancy, following:

$$Đ_i = Đ_i(0)(1 - \theta_1 - \theta_2 - \ldots - \theta_n) \quad (5)$$

Such behaviour is exhibited, for example, for diffusion of CF_4 in MFI zeolite.[16]

A site-to-site jump leaves behind a vacancy. Subsequent jumps are more likely to fill this vacancy, thus producing "vacancy correlation" effects. An important consequence of vacancy correlations is that the self-diffusivities are reduced. When the jump of species i creates a vacancy and this vacancy is filled by species j, the vacancy correlation effect is captured by the term containing the "exchange" coefficients $Đ_{ij}$ in eqn. (3). The Onsager reciprocal relations demand $Đ_{ij} = Đ_{ji}$. The net effect of this exchange is a slowing down of a faster moving species due to interactions with a species of lower mobility. Also, a species of lower mobility is accelerated by interactions with another species of higher mobility. When the jump of species i creates a vacancy and this vacancy is filled by species i itself, the correlation effect is described by $Đ_{ii}$; this must be expected to be identical to the pure component M–S diffusivity $Đ_i$.

For structures such as MFI, consisting of a three-dimensional network of intersecting straight and zig-zag channels, additional correlation effects arise due to geometric effects and due to "ballistic" jumps that begin and end at sites that are not nearest neighbours.[17–19]

The estimation of the exchange coefficients $Đ_{ij}$ is a key issue in the proper description of mixture diffusion and, in particular self-diffusivities that are strongly influenced by correlation effects. In general we may expect the interchange between species species i and species j to be dictated by the mobilities of the pure species and their compositions in the mixture:

$$Đ_{ij} = f\left(Đ_i, Đ_j, \frac{\theta_i}{\theta_i+\theta_j}, \frac{\theta_j}{\theta_i+\theta_j}\right) \quad (6)$$

Drawing inspiration from diffusion in fluid mixtures, Krishna and Wesselingh[12] suggested the logarithmic interpolation formula:

$$Đ_{ij} = [Đ_i]^{\theta_i/(\theta_i+\theta_j)}[Đ_j]^{\theta_j/(\theta_i+\theta_j)} \quad (6a)$$

This formula was found to predict the *transport* diffusivities in *binary* mixtures in MFI with reasonable accuracy.[14]

Alternatively, we may postulate a linear interpolation formula

$$Đ_{ij} = \frac{\theta_i}{(\theta_i+\theta_j)}[Đ_i] + \frac{\theta_j}{(\theta_i+\theta_j)}[Đ_j] \quad (6b)$$

or assume that the interchange process is composition independent, obeying say the square root formula

$$Đ_{ij} = [Đ_i Đ_j]^{1/2} \quad (6c)$$

For facile particle–particle exchange, vacancy correlation effects tend to get washed out; this is described by

$$Đ_{ij} \to \infty \quad (6d)$$

Facile counter-exchange of molecules could occur, for example, within the cages of FAU and LTA zeolites when intra-cage hopping rates are high. When $Đ_{ij} \to \infty$, eqn. (3) simplify to give a set of *uncoupled* flux equations:

$$N_i = -\rho\Theta_{i,\mathrm{sat}}Đ_i\frac{\theta_i}{RT}\nabla\mu_i; \quad i = 1,2,\ldots n \quad (7)$$

Self-diffusivities are more significantly influenced by correlation effects than are the transport diffusivities and therefore provide more stringent tests for the applicability of eqn. (6a), (6b), (6c) or (6d).

The chemical potential gradients in eqn. (3) may be expressed in terms of the gradients of the occupancies by introduction of the matrix of thermodynamic factors [Γ]

$$\frac{\theta_i}{RT}\nabla\mu_i = \sum_{j=1}^{n}\Gamma_{ij}\nabla\theta_j; \quad \Gamma_{ij} \equiv \left(\frac{\Theta_{j,\mathrm{sat}}}{\Theta_{i,\mathrm{sat}}}\right)\frac{\Theta_i}{p_i}\frac{\partial p_i}{\partial\Theta_j}; \quad i,j = 1,2\ldots n \quad (8)$$

Knowledge of the sorption isotherm is sufficient to allow estimation of [Γ] and $\nabla(\mu)$. If the n-component sorption can be described by the multicomponent Langmuir isotherm, the elements of [Γ] are given by

$$\Gamma_{ij} = \delta_{ij} + \frac{\theta_i}{1 - \theta_1 - \theta_2 - \ldots - \theta_n}; \quad i,j = 1,2\ldots n \quad (9)$$

where δ_{ij} is the Kronecker delta.

It is convenient to define a n-dimensional square matrix [B] with elements

$$B_{ii} = \frac{1}{Đ_i} + \sum_{\substack{j=1\\ j\neq i}}^{n}\frac{\theta_j}{Đ_{ij}}; \quad B_{ij} = -\frac{\theta_i}{Đ_{ij}}; \quad i,j = 1,2\ldots n \quad (10)$$

With this definition of [B], eqn. (3) can be cast into n-dimensional matrix form:

$$(N) = -\rho[\Theta_{\mathrm{sat}}][B]^{-1}[\Gamma]\nabla(\theta) \quad (11)$$

which gives the following expressions for the Fick matrix

$$[D] = [B]^{-1}[\Gamma] \quad (12)$$

Measurements of self-diffusivities are commonly made by labelling (*i.e.* tracing) species 1 and monitoring it during the diffusion process. Therefore, to determine the self-diffusivity of component 1 in say a ternary mixture consisting of species 1, 2 and 3 we consider a *quaternary* system made up of species 1, 2, 3 and 4 where species 4 is the labelled species 1. The total number of molecules of 1 and 4 are held constant during the diffusion process, and therefore we have the constraint:

$$\nabla\theta_4 = \nabla\theta_{1^*} = -\nabla\theta_1 \quad (13)$$

Furthermore, during self-diffusivity measurements of component 1, there are no concentration gradients for species 2 and 3, *i.e.*

$$\nabla\theta_2 = 0; \quad \nabla\theta_3 = 0 \quad (14)$$

During tracer diffusion we essentially have equimolar diffusion of component 1 and its labelled form, *i.e.* component 4, giving:

$$N_1 = -N_4 = -N_{1^*} \quad (15)$$

Applying the constraints (13) and (14) to eqn. (11) we obtain

$$N_1 = -\rho\Theta_{1,\mathrm{sat}}(D_{11} - D_{14})\nabla\theta_1 = -\rho\Theta_{1,\mathrm{sat}}D_1^*\nabla\theta_1 \qquad (16)$$

where D_{11} and D_{14} are the (1,1) and (1,4) elements of the Fick matrix [D]. Eqn. (16) also serves to define the self (or tracer) diffusivity of component 1, D_1^*; this diffusivity is identical to $D_{1^*}^*$, defined by

$$N_4 = N_{1^*} = -\rho\Theta_{1,\mathrm{sat}}(D_{44} - D_{41})\nabla\theta_4 = -\rho\Theta_{1,\mathrm{sat}}D_{1^*}^*\nabla\theta_{1^*} \qquad (17)$$

because 1 and 4 are the same molecular species. The exchange coefficient $Đ_{14}$ when estimated using eqn. (6) is identical with the pure component M–S diffusivity of component 1, *i.e.* $Đ_{14} = Đ_{11}$. Furthermore, since species 4 is the tracer component its concentration in the mixture is vanishingly small, *i.e.* $\theta_4 \to 0$.

Calculating the elements of [D] using eqn. (12), after introducing the various simplifications for tracer diffusion outlined above, we obtain the following simple and elegant expression for D_1^*:

$$D_1^* \equiv D_{11} - D_{14} = \frac{1}{\dfrac{1}{Đ_1} + \dfrac{\theta_1}{Đ_{11}} + \dfrac{\theta_2}{Đ_{12}} + \dfrac{\theta_3}{Đ_{13}}} \qquad (18)$$

It is clear from eqn. (18) that the self-diffusivity is strongly influenced by particle–particle exchanges $Đ_{12}$ and $Đ_{13}$. Eqn. (18) may be extended to a general n-component mixture:

$$D_1^* = \frac{1}{\dfrac{1}{Đ_1} + \dfrac{\theta_1}{Đ_{11}} + \dfrac{\theta_2}{Đ_{12}} + \dfrac{\theta_3}{Đ_{13}} + \ldots\ldots\dfrac{\theta_n}{Đ_{1n}}} \qquad (19)$$

Eqn. (6) provides a procedure for estimation of the various exchange coefficients, $Đ_{ij}$ and, in conjunction with eqn. (4) or (5), eqn. (19) relates the self-diffusivity D_1^* to the zero-loading diffusivities $Đ_i(0)$. By rotating the subscripts in eqn. (19), analogous expressions are obtained for the self-diffusivities of components 2, 3,...n. The expression (19) reduces for a single component system to

$$D_1^* = \frac{1}{\dfrac{1}{Đ_1} + \dfrac{\theta_1}{Đ_{11}}} \qquad (20)$$

that was derived earlier.[11] For a binary mixture, the formula (19) simplifies to

$$D_1^* = \frac{1}{\dfrac{1}{Đ_1} + \dfrac{\theta_1}{Đ_{11}} + \dfrac{\theta_2}{Đ_{12}}} \qquad (21)$$

We note, in passing, that the expression derived earlier in ref. 8 for self-diffusivity in a binary mixture is flawed as a consequence of an incorrect derivation. It is important to stress that the expression for the self-diffusivity (19) is not influenced by the thermodynamic correction factor [Γ]. Put another way, sorption thermodynamics play no role in the determination of the self-diffusivity.

3. KMC simulation methodology

We first perform KMC simulations in which each component follows Langmuir isotherm behaviour. We assume the lattice to be made up of equal sized sites that can be occupied by only one molecule at a time. Particles can move from one site to a neighbouring site *via* hops. Two types of topologies were studied: (a) square lattice, and (b) MFI; see Fig. 1. For the square lattice (Fig. 1(a)) we take the distance of separation between adjacent sites to be unity, $l = 1$. Furthermore the jump frequency of species 1 is taken to be equal in all directions and set to unity, *i.e.*, $\nu_1 = 1\ \mathrm{s}^{-1}$. The jump frequency of component 2 is taken to be sixteen times that of component 1. For the MFI topology, the jump frequencies along the straight and zig-zag channels for component 1 are taken to correspond to that for 2-methyl hexane (2MH) at 300 K, $\nu_{1,\mathrm{str}} = 1.4 \times 10^5\ \mathrm{s}^{-1}$; $\nu_{1,\mathrm{zz}} = 5 \times 10^4\ \mathrm{s}^{-1}$; these values were calculated by Smit *et al.* using the transition state theory.[20] The maximum loading was taken to be 4 molecules per unit cell, where the molecules are all located at the intersections. We have published the details of the pure component 2MH simulations earlier;[10] these simulations have established the validity of eqn. (5) to describe the variation of the jump diffusivity $Đ_i$ with occupancy. The jump frequencies for the other components 2 and 3 are taken to be, respectively, twice and half, the corresponding values for component 1; Table 1 summarises the jump frequencies and the zero-loading jump diffusivities for all three components.

Table 1 Transition probabilities and zero-loading diffusivities for a three-component system

Species, i	$\Theta_{i,\mathrm{sat}}$	$\nu_{\mathrm{zz}}/\mathrm{s}^{-1}$	$\nu_{\mathrm{str}}/\mathrm{s}^{-1}$	$Đ_i(0)/\mathrm{m}^2\ \mathrm{s}^{-1}$
1 (= 2MH)	4	5×10^4	1.4×10^5	6.85×10^{-14}
2	4	1×10^5	2.8×10^5	13.7×10^{-14}
3	4	2.5×10^4	7×10^4	3.43×10^{-14}

We employ a standard KMC methodology to propagate the system (details in ref. 10, 21 and 22). A hop is made every KMC step and the system clock is updated with variable time steps. For a given configuration of random walkers on the lattice a process list containing all possible M moves to vacant intersection sites is created. Each possible move i is associated with a transition probability ν_i. Now, the mean elapsed time τ is the inverse of the total rate coefficient

$$\tau^{-1} = \nu_{\mathrm{total}} = \sum_{i=1}^{M} \nu_i \qquad (22)$$

which is then determined as the sum over all processes contained in the process list. The actual KMC time step Δt for a given configuration is randomly chosen from a Poisson distribution

$$\Delta t = -\ln(u)/\nu_{\mathrm{total}} \qquad (23)$$

where $u \in [0,1]$ is a uniform random deviate. The time step Δt is independent of the chosen hopping process. To select the actual jump, we define process probabilities according to $p_i = \sum_{j=1}^{i} \nu_j/\nu_{\mathrm{total}}$. The ith process is chosen, when $p_{i-1} < \gamma < p_i$, where $\gamma \in [0,1]$ is another uniform random deviate. After having performed a hop, the process list is updated. In order to avoid wall effects we employ periodic boundary conditions. We have investigated the finite size effect on the diffusivity and found systems of 10×10 and $5 \times 5 \times 5$ unit cells for the square lattice and MFI topologies, respectively, to be sufficiently large and giving satisfactory results.[10,14] From the KMC simulations we calculate the self-diffusivity of each of the three components from the mean square displacement of the individual particles:

$$D_i^* = \frac{1}{6}\lim_{\Delta t \to \infty} \frac{1}{\Delta t}\frac{1}{N_i}\sum_{j=1}^{N_i} \left\langle \left(\boldsymbol{r}_{i,j}(t + \Delta t) - \boldsymbol{r}_{i,j}(t)\right)^2 \right\rangle \qquad (24)$$

where $\langle \cdots \rangle$ denotes both ensemble and time averaging over the entire system trajectory; N_i is the number of particles belong to species i; $r_{i,j}(t)$ is the position vector at time t.

Applying linear response theory, the Onsager transport coefficients L_{ij} can be determined using the displacement formula

$$L_{ij} = \lim_{\Delta t\to\infty} L_{ij}(\Delta t) = \frac{1}{6}\frac{1}{N_s}\lim_{\Delta t\to\infty}\frac{1}{\Delta t}\left\langle\left(\sum_{l=1}^{N_i}\left(\boldsymbol{r}_{l,i}(t+\Delta t)-\boldsymbol{r}_{l,i}(t)\right)\right)\times\left(\sum_{k=1}^{N_j}\left(\boldsymbol{r}_{k,j}(t+\Delta t)-\boldsymbol{r}_{k,j}(t)\right)\right)\right\rangle \quad (25)$$

In contrast to the formula for L_{ij} used by Sanborn and Snurr[23] in their MD simulations, the normalising volume is replaced by N_s, the total number of discrete adsorption sites in the simulation. Eqn. (25) yields the L_{ij} in units of $m^2\ s^{-1}$ and they are related to the Fick [D] by the formula derived in our earlier publication[14]

$$[D] = [L]\begin{bmatrix} 1/\theta_1 & 0 & 0 \\ 0 & \ddots & 0 \\ 0 & 0 & 1/\theta_n \end{bmatrix}[\Gamma] = [B]^{-1}[\Gamma] \quad (26)$$

The Onsager coefficients L_{ij} are subject to strong correlation effects and therefore the obtained values of the transport coefficients vary strongly with the separation time between two configurations Δt; a Δt of 10^{-3} s was employed, on the basis of our previous experience.[10,14]

4. Verification of self-diffusivity model

4.1 Binary mixtures

Let us first consider KMC simulations for the square lattice with a binary mixture with jump frequencies $\nu_1 = 1$; $\nu_2/\nu_1 = 16$. The total occupancy of the system is fixed as $\theta_1 + \theta_2 = 0.96$. Simulations were carried out for various mole fractions of component 1 in the mixture; the results are presented as open symbols in Fig. 2(a) and (b). The calculations using eqn. (21) in conjunction with eqn. (5) and the four variants of eqn. (6) are also shown in Fig. 2. As expected, the facile exchange model is hopelessly in error; this model ignores the strong correlations that influence self-diffusivities. Of the three other mixture rules for the exchange coefficient, the square root model, eqn. (6c) does not portray the right limiting values for the diffusivities. The logarithmic and linear interpolation formulae both show the proper limiting behaviour. The logarithmic interpolation formula is superior to the linear interpolation formula in its predictive capability for component 2, that is strongly decelerated by the slower moving 1.

In Fig. 3 we present the KMC simulation results for the elements of the Onsager matrix [L] for the same system as above. We see that the predictions of eqn. (26) using the logarithmic interpolation formula eqn. (6a) is clearly superior to that of the other scenarios for exchange. In particular the cross-coefficient L_{12} is predicted extremely well. It is interesting to note that though the predictions of Onsager [L] using eqn. (6a) are extremely good, the corresponding predictions of self-diffusivities (Fig. 2) are less good, emphasising the fact that correlations affect *self-diffusivities* to a much greater extent than *transport* diffusivities.

Next we consider the experimental data of Schuring *et al.*[9] for self-diffusivities in the mixture of n-hexane (nC6, component 1) and 2-methylpentane (2MP, component 2) in MFI zeolite at a temperature $T = 433$ K and total pressure $P = 6.6$ kPa. In Fig. 4(a) the experimental data are compared with the self-diffusivities calculated using eqn. (5), (6a) and (21). The sharp decrease in the self-diffusivity of nC6 with increasing 2MP loading is portrayed very well by the model. In Fig. 4(b) we compare the self-diffusivity calculations for nC6 using four different scenarios for the estimation of the exchange coefficient, eqn. (6a), (6b), (6c) or (6d). The facile exchange assumption is hopelessly in error. The square root model predictions are good for low 2MP loadings but do not show the proper trend with higher 2MP loadings. Both the linear and logarithmic interpolation formulae show the right limiting behaviour but the linear interpolation formula shows significant deviations at intermediate composition ranges. Only the logarithmic interpolation formula is successfully able to predict the right trend over the entire composition range. These findings are consonant with those obtained from Fig. 2(b) for the square lattice simulations.

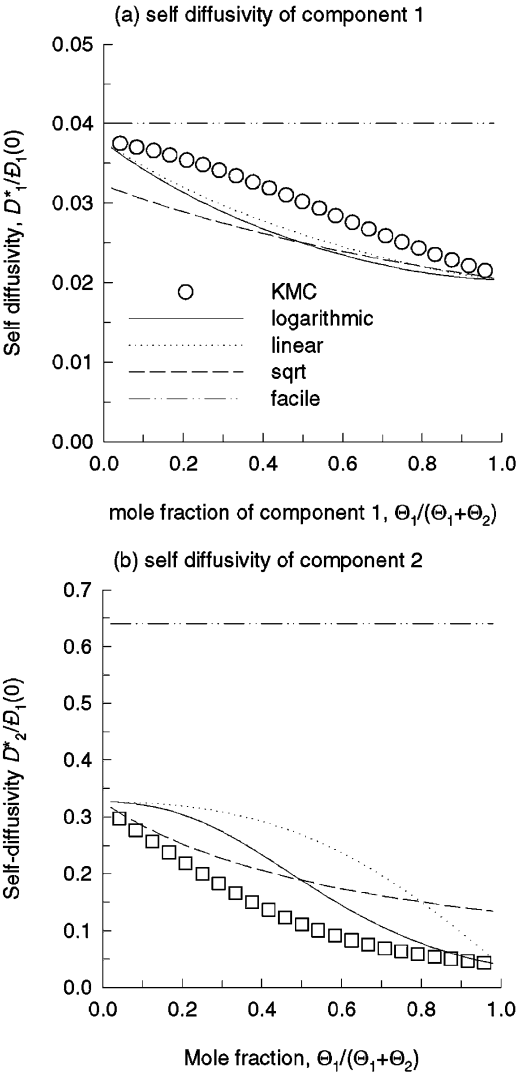

Fig. 2 KMC simulations of the self-diffusivities for binary mixture in a square lattice. The total occupancy of the lattice is 0.96. The lattice parameters are $l = 1$ and the jump frequency of component 1, $\nu_1 = 1$ and that of component 2, $\nu_2 = 16$. The Onsager coefficient has been normalised with respect to the zero-loading diffusivity value $Đ_1(0)$. The KMC simulation results are compared with predictions using eqn. (5), (6) and (21). Four different methods for estimation of the exchange coefficient, using either eqn. (6a), (6b), (6c) or (6d) are compared.

Consider now the MD simulations of Snurr and Kärger[4] for self-diffusivities in a mixture of CH_4 (component 1) and CF_4 (component 2) in MFI zeolite at 200 K. The MD simulations were carried out at a total mixture loading of $\Theta_1 + \Theta_2 = 12$ molecules per unit cell and the methane loading is varied from 0–12 molecules per unit cell; their simulation data are shown as open symbols in Fig. 5. We will try to calculate the self-diffusivities from pure component data. The pure component diffusivities at zero loading are estimated as $Đ_1(0) = 60 \times 10^{-10}\ m^2$

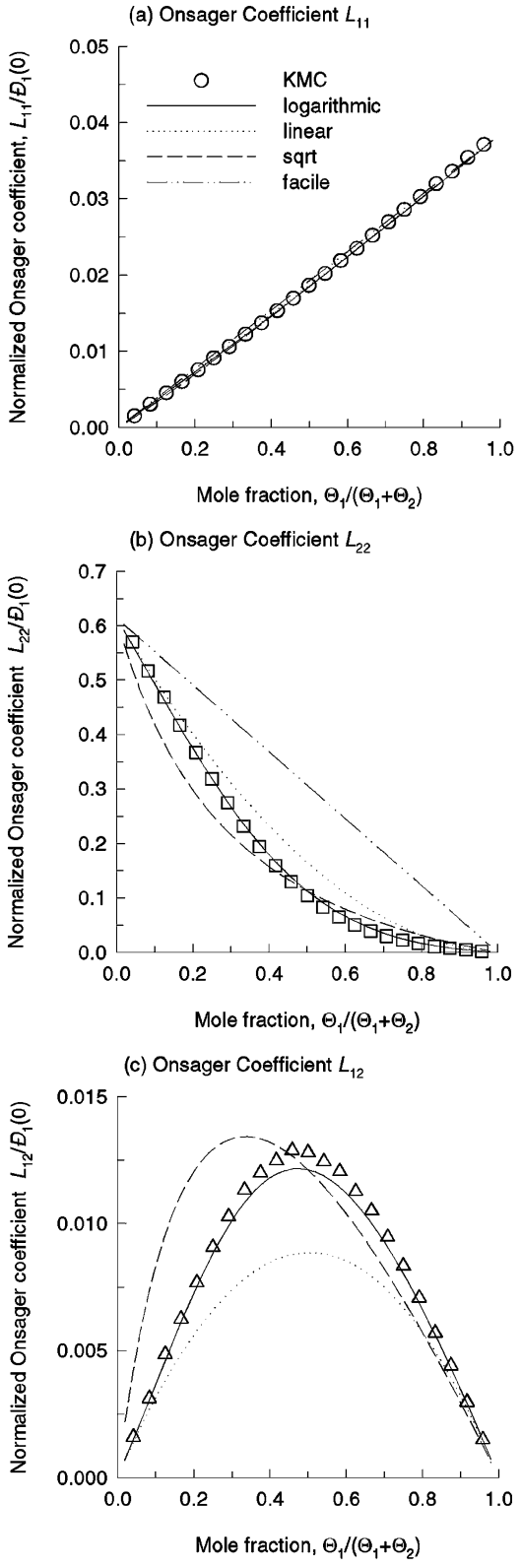

Fig. 3 KMC simulations of the self-diffusivities for binary mixture, of varying composition, in a square lattice. The total occupancy of the lattice is 0.96. The lattice parameters are $l = 1$ and the jump frequency of component 1, $\nu_1 = 1$ and that of component 2, $\nu_2 = 16$. The Onsager coefficient has been normalised with respect to the zero-loading diffusivity value $Đ_1(0)$. The markers are the KMC simulations and the continuous lines represent using eqn. (26). Four different methods for estimation of the exchange coefficient, using either eqn. (6a), (6b), (6c) or (6d) are compared.

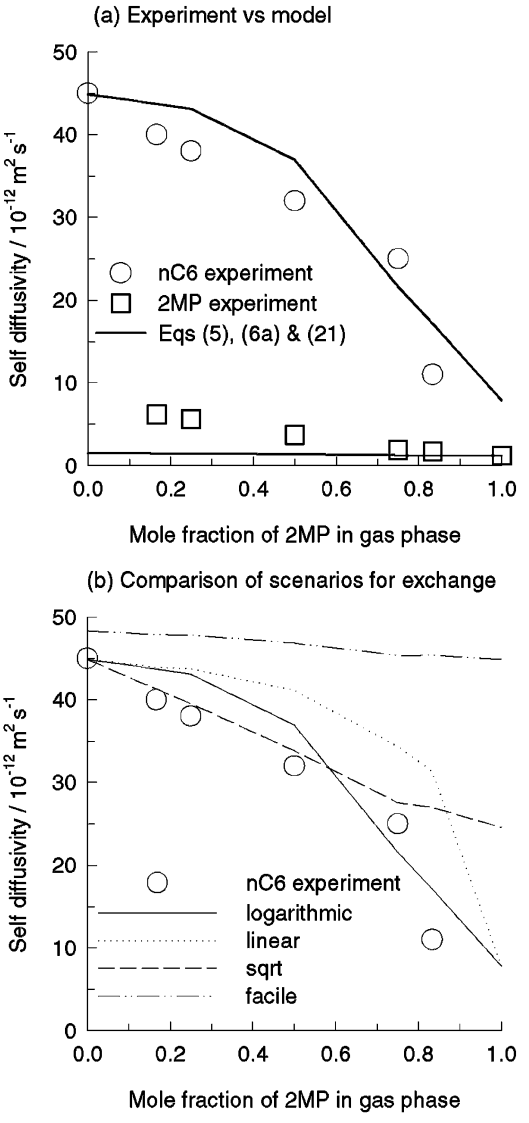

Fig. 4 (a) Experimental data of Schuring *et al.*[9] for self-diffusivities in MFI of the mixture of n-hexane (nC6, component 1) and 2-methylpentane (2MP, component 2) are compared with calculations using eqn. (5), (6a) and (21). The temperature $T = 433$ K and total pressure $P = 6.6$ kPa. (b) Self-diffusivity of nC6 calculated using four different models for estimation of the exchange coefficient, using either eqn. (6a), (6b), (6c) or (6d). The calculations were performed taking $Đ_1(0) = 52.5 \times 10^{-12}$; $Đ_2(0) = 1.61 \times 10^{-12}$ m^2 s^{-1}. The component loadings at various 2MP gas phase compositions were taken from experimental data reported in Fig. 6 of Schuring *et al.*[9] The saturation loadings are $\Theta_{1,\mathrm{sat}} = 8$ and $\Theta_{1,\mathrm{sat}} = 4$ molecules per unit cell.

s^{-1}, $Đ_2(0) = 25 \times 10^{-10}$ m^2 s^{-1}. Methane being a smaller molecule has a higher saturation loading than that of CF_4; we therefore take $\Theta_{1,\mathrm{sat}} = 22$ and $\Theta_{2,\mathrm{sat}} = 12$ on the basis of information on mixture isotherms.[24] The calculations of the diffusivities $Đ_1^*$ and $Đ_2^*$ using eqn. (5), (6) and (21) are also shown in Fig. 5 for four different scenarios for the estimation of the exchange coefficients. Clearly, the assumption of facile exchange is not valid. All the other mixture rules give comparable results and in very good agreement with the MD simulation results.

Gergidis and Theodorou[6] have performed two sets of MD simulations for the self-diffusivities in mixture of CH_4 (1) and n-butane (2) at 300 K in MFI; see Fig. 6. In the first set (Fig. 6(a)) the n-butane loading Θ_2 is kept constant at 4 molecules per unit cell and the methane loading Θ_1 is varied. In the second set (see Fig. 6(b)) the methane loading Θ_1 is kept constant at 4 molecules per unit cell and the n-butane loading Θ_2 is varied. We now attempt to model the self-diffusivities using the M–S formulations developed above. The saturation loadings are estimated as $\Theta_{1,\mathrm{sat}} = 22$ and $\Theta_{2,\mathrm{sat}} = 12$. The pure component diffusivities at 300 K are taken as

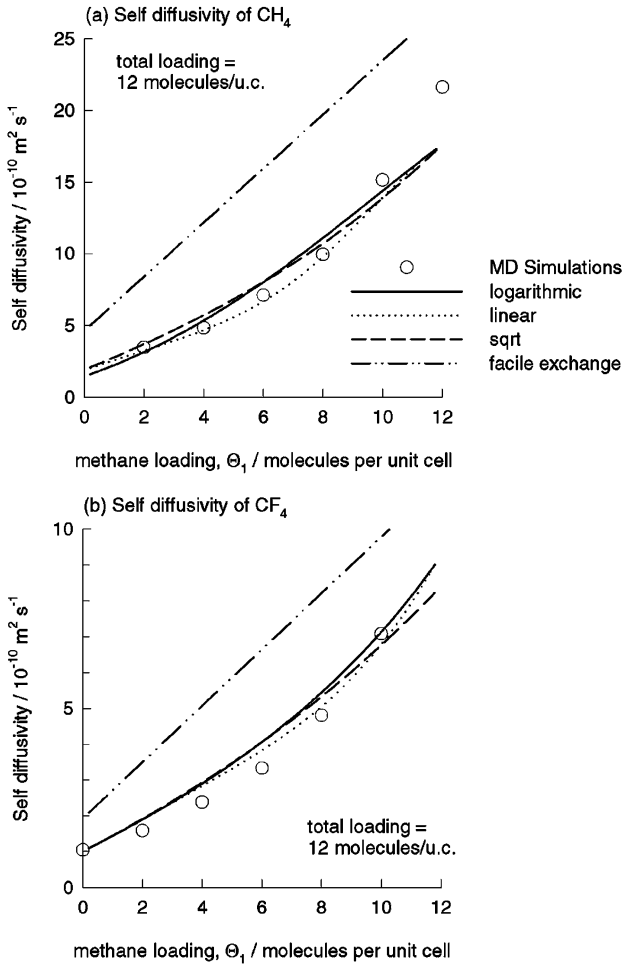

Fig. 5 Comparison of MD binary mixture simulations of Snurr and Kärger[4] for (a) CH_4 and (b) CF_4 in MFI at 200 K with calculations using eqn. (5), (6) and (21). Four different methods for estimation of the exchange coefficient, using either eqn. (6a), (6b), (6c) or (6d) are compared. The calculations were performed taking $Đ_1(0) = 60 \times 10^{-10}$ m^2 s^{-1}, $Đ_2(0) = 25 \times 10^{-10}$ m^2 s^{-1}. The saturation loadings are $\Theta_{1,\mathrm{sat}} = 22$ and $\Theta_{1,\mathrm{sat}} = 13$ molecules per unit cell.

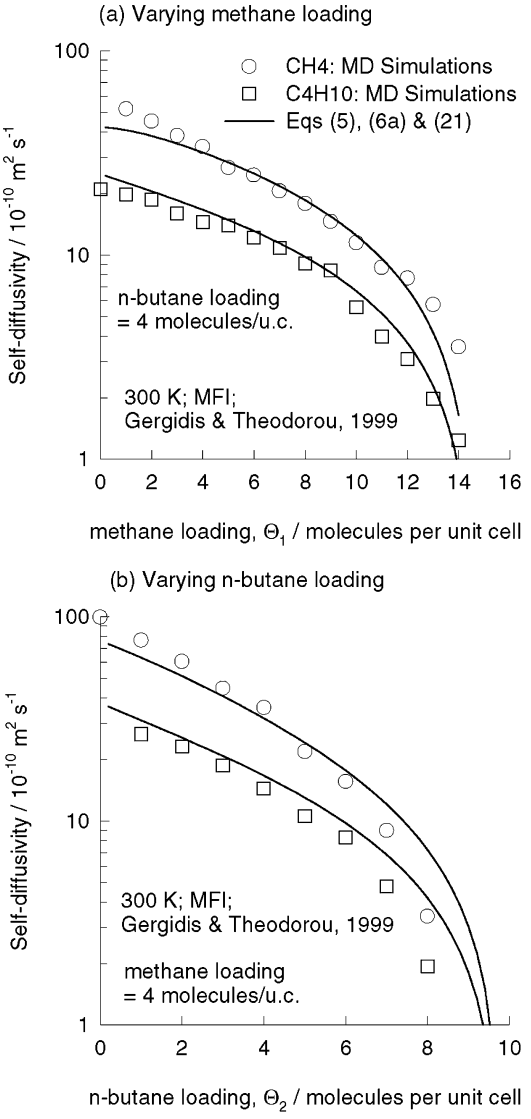

Fig. 6 Comparison of MD binary mixture simulations of Gergidis and Theodorou[6,7] for the mixture of CH_4 (1) and n-butane (2) in MFI at 300 K with calculations using eqn. (5), (6a) and (21). The calculations were performed taking $Đ_1(0) = 11 \times 10^{-9}$ m^2 s^{-1} and $Đ_2(0) = 5 \times 10^{-9}$ m^2 s^{-1}. The saturation loadings are $\Theta_{1,\mathrm{sat}} = 22$ and $\Theta_{1,\mathrm{sat}} = 12$ molecules per unit cell.

$Đ_1(0) = 11 \times 10^{-9}$ m^2 s^{-1} and $Đ_2(0) = 5 \times 10^{-9}$ m^2 s^{-1} on the basis of the data presented by Gergidis and Theodorou.[6] The calculations of the diffusivities in the mixture, $Đ_1^*$ and $Đ_2^*$ using eqn. (5), (6a) and (21) show good agreement with the MD simulations for both simulation sets.

4.2 Ternary mixtures

We now turn to self-diffusivities in ternary mixtures in MFI zeolite using the data summarized in Table 1. In the first series of KMC simulations with the ternary mixture, we keep the mixture composition constant and $\theta_1 = \theta_3 = \theta_3 = 0.333$ for each species and study the influence of varying the total occupancy $(\theta_1 + \theta_3 + \theta_3)$. The KMC simulation results for the $Đ_i^*$ are shown in Fig. 7(a) as open symbols. Calculations of $Đ_i^*$ using eqn. (18), in conjunction with eqn. (5) and (6a), are shown in Fig. 6(a) as continuous lines. The agreement of KMC simulations with the expression (18) is excellent. If all the particle–particle exchange process is assumed to take place infinitely fast, *i.e.* $Đ_{ij} \to \infty$, the calculations using eqn. (18) are significantly worse, especially for the faster moving 2 and 3; see Fig. 6(b). Put another way, correlation effects tend to affect the faster moving species to a greater extent than the slower moving species.

Next, we performed a set of three KMC simulations in which the total occupancy was held constant $(\theta_1 + \theta_3 + \theta_3 = 0.48)$ but the mixture compositions were varied. In Fig. 8(a) we present the simulation results which were carried out for an equimolar mixture of 2 and 3 in which the mole fraction of component 1, $\theta_1/(\theta_1 + \theta_3 + \theta_3)$ was varied from 0 to 1. The continuous lines in Fig. 8(a) were calculated using eqn. (18), along with eqn. (5) and (6a). The predictions for the species 1 and 3 are good while the predictions for the fastest moving species 2 are significantly less good. This is because the fastest moving species is affected more by correlation effects and these effects are apparently not entirely captured by the logarithmic interpolation formula. Geometric correlations exist in practice[7] and these are picked up by KMC simulations but not entirely by the assumption of isotropy implied by our use of the Maxwell–Stefan equations.

Similar conclusions can be drawn from two further ternary KMC simulation results presented in Fig. 8(b) and (c) wherein the compositions of components 2 and 3 are varied in equimolar mixtures of the remaining two components.

The inability of eqn. (6a) to mirror all correlation effects present during diffusion in MFI zeolite, is less crucial in the prediction of the *transport* coefficients. In order to demonstrate

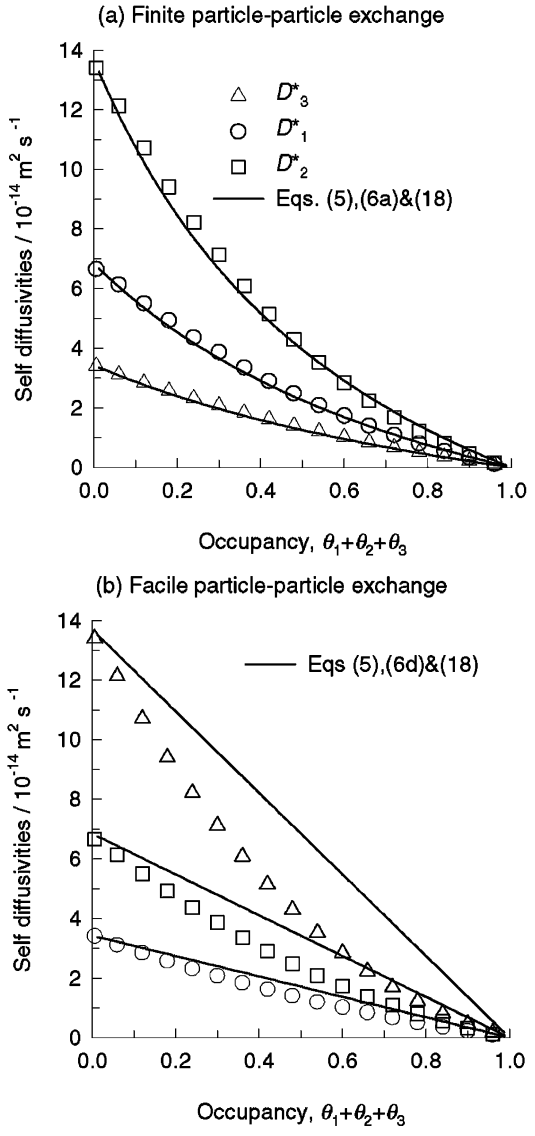

Fig. 7 KMC simulations for self-diffusivity in ternary mixture as function of total occupancy ($\theta_1 + \theta_3 + \theta_3$). In these simulations we keep $\theta_1 = \theta_3 = \theta_3 = 0.333$ for each species. The pure component parameters are specified in Table 1. The KMC simulation results are shown as open symbols. The continuous lines in (a) and (b) are obtained using eqn. (5), (6a) and (18).

this we present in Fig. 9 the KMC simulation results for the elements of the Onsager matrix [L] for a ternary mixture in which the mole fraction of component 3 is varied in a mixture where the compositions of the remaining two components 1 and 2 are equimolar. The total occupancy was held constant ($\theta_1 + \theta_3 + \theta_3 = 0.48$). The calculations of the diagonal elements of [L] using eqn. (26) and the logarithmic interpolation formula are in excellent agreement. The predictions of the cross coefficients are only somewhat less good, especially for the elements L_{13} and L_{23}.

5. Conclusions

We have derived a simple analytical expression (eqn. (19)) for the self-diffusivity of a component in a multicomponent mixture in zeolites. The expression for the self-diffusivity contains various exchange coefficients $Đ_{ij}$ that portray correlations in molecular jumps. Four different scenarios are postulated for the estimation of these exchange coefficients. By comparison with KMC and MD simulations, and experimental data, on

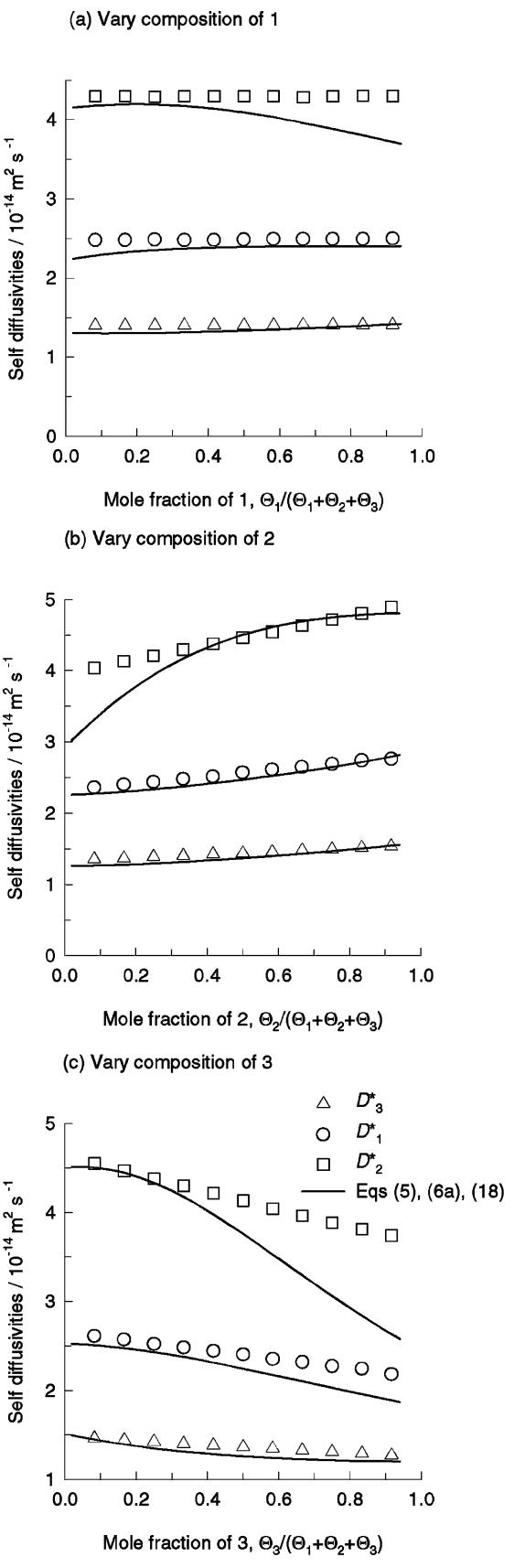

Fig. 8 KMC simulations for self-diffusivities in ternary mixture as function of mole fraction of either component 1, 2 or 3. In each case the mole fractions of the other two components are taken equal. In all cases the total occupancy ($\theta_1 + \theta_3 + \theta_3$) is kept constant at 0.48. The pure component parameters are specified in Table 1. The KMC simulation results for the D_i^* are shown as open symbols. The continuous lines are obtained using eqn. (5), (6a) and (18).

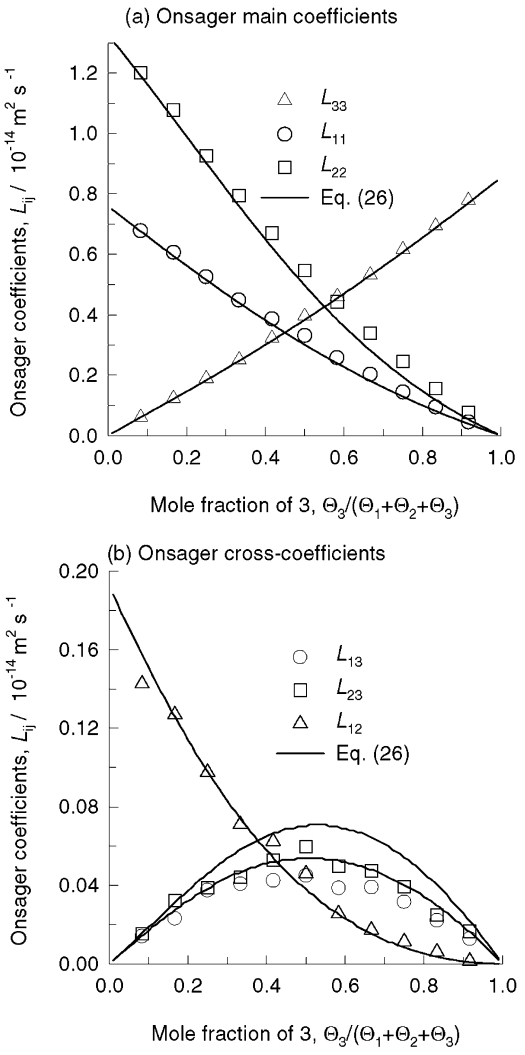

Fig. 9 KMC simulations for L_{ij} in ternary mixture as function of mole fraction of component 3, $\theta_3/(\theta_1+\theta_3+\theta_3)$ with the total occupancy kept constant $(\theta_1+\theta_3+\theta_3)=0.48$. The mixture is equimolar in species 1 and 2. The pure component parameters are specified in Table 1. The KMC simulation results for the L_{ij} are shown as open symbols. The continuous lines are obtained using eqn. (26) wherein the exchange coefficients have been estimated using the logarithmic interpolation formula (6a).

binary and ternary mixtures, the following conclusions can be drawn:

Eqn. (19) provides a good estimate of the self-diffusivities in multicomponent mixtures for a variety of loadings and compositions provided the exchange coefficients are estimated using the logarithmic interpolation formula (6a).

The assumption of facile exchange, *i.e.* ignoring correlation effects (by effectively taking $Đ_{ij}\rightarrow\infty$), leads to extremely poor predictions of the self-diffusivities.

Correlation effects affect the *transport* coefficients to a lesser extent than they do the *self-diffusivities* and the predictions of the Onsager matrix [L] using eqn. (26) are of good accuracy.

We conclude that the Maxwell–Stefan theory for multicomponent diffusion in zeolites can be used to predict self and transport diffusivities with good accuracy from *pure* component transport data.

Acknowledgement

RK and DP acknowledge a grant *Programmasubsidie* from the Netherlands Foundation for Fundamental Research (CW-NWO) for development of novel concepts in reactive separations.

References

1 J. Kärger and D. M. Ruthven, *Diffusion in Zeolites and Other Microporous Solids*, Wiley, New York, 1992.
2 D. M. Ruthven and M. F. M. Post, in *Introduction to Zeolite Science and Practice*, ed. H. van Bekkum, E. M. Flanigan and J. C. Jansen, Elsevier, Amsterdam, 2nd edn., 2000, ch. 12, pp. 525–578.
3 D. M. Ruthven, *Principles of Adsorption and Adsorption Processes*, Wiley, New York, 1984.
4 R. Q. Snurr and J. Kärger, *J. Phys. Chem. B.*, 1997, **101**, 6469.
5 S. Jost, N. K. Bär, S. Fritzsche, R. Haberlandt and J. Kärger, *J. Phys. Chem. B*, 1998, **102**, 6375.
6 L. N. Gergidis and D. N. Theodorou, *J. Phys. Chem. B.*, 1999, **103**, 3380.
7 L. N. Gergidis, D. N. Theodorou and H. Jobic, *J. Phys. Chem. B.*, 2000, **104**, 5541.
8 D. Paschek and R. Krishna, *Langmuir*, 2001, **17**, 247.
9 D. Schuring, A. O. Koriabkina, A. M. de Jong, B. Smit and R. A. van Santen, *J. Phys. Chem. B.*, 2001, **105**, 7690–7698.
10 D. Paschek and R. Krishna, *Phys. Chem. Chem. Phys.*, 2000, **2**, 2389–2394.
11 D. Paschek and R. Krishna, *Chem. Phys. Lett.*, 2001, **333**, 278–284.
12 R. Krishna and J. A. Wesselingh, *Chem. Eng. Sci.*, 1997, **52**, 861–911.
13 F. Kapteijn, J. A. Moulijn and R. Krishna, *Chem. Eng. Sci.*, 2000, **55**, 2923–2930.
14 D. Paschek and R. Krishna, *Phys. Chem. Chem. Phys.*, 2001, **3**, 3185–3191.
15 E. J. Maginn, A. T. Bell and D. N. Theodorou, *J. Phys. Chem.*, 1993, **97**, 4173–4181.
16 A. I. Skoulidas and D. S. Sholl, *J. Phys. Chem. B.*, 2001, **105**, 3151–3154.
17 J. Kärger, *J. Phys. Chem.*, 1991, **95**, 5558–5560.
18 J. Kärger, P. Demontis, G. B. Suffritti and A. Tilocca, *J. Chem. Phys.*, 1999, **110**, 1163–1172.
19 F. Jousse, S. M. Auerbach and D. P. Vercauteren, *J. Chem. Phys.*, 2000, **112**, 1531–1540.
20 B. Smit, L. D. J. C. Loyens and G. L. M. M. Verbist, *Faraday Discuss.*, 1997, **106**, 93–104.
21 S. M. Auerbach, *Int. Rev. Phys. Chem.*, 2000, **19**, 155–198.
22 M. O. Coppens, A. T. Bell and A. K. Chakraborty, *Chem. Eng. Sci.*, 1999, **54**, 3455–3463.
23 M. J. Sanborn and R. Q. Snurr, *Sep. Purif. Technol.*, 2000, **20**, 1–13.
24 M. Heuchel, R. Q. Snurr and E. Buss, *Langmuir*, 1997, **13**, 6795–6804.